

DESIGN OF JACKFRUIT GUM-BASED GENIPIN CROSSLINKED NANOPARTICLES FOR SUSTAINED RELEASE OF CURCUMIN: OPTIMIZATION AND *IN VITRO* CHARACTERIZATION

SWAPNIL THAKARE and ASHISH GORLE

Department of Pharmaceutics, R. C. Patel Institute of Pharmaceutical Education and Research, Shirpur 425 405, Maharashtra, India

✉ *Corresponding author: A. P. Gorle, ashishgorle@rediffmail.com*

Received October 30, 2023

The present work aims to design jackfruit gum-based curcumin-loaded nanoparticles (CUR-NPs) for improved drug entrapment and modified release of CUR using ionotropic gelation. Briefly, the optimization of CUR-NPs was confirmed using a 3² response surface methodology. The diffractogram and thermogram of CUR-NPs confirmed reduction of crystallinity of CUR (optimized batch: F5) due to jackfruit gum and genipin cross-linked polymeric network. The particle size and zeta potential analysis confirmed formation of nanosized and stable CUR-NPs, respectively. Also, the nanoparticles demonstrated $83.99 \pm 1.23\%$ entrapment efficiency, whereas they showed $98.36 \pm 0.96\%$ of CUR release within 12 h at pH 7.4. The CUR-NPs exhibited good mucoadhesive properties due to the presence of jackfruit gum. Finally, the MTT assay showed a decrease in colorectal cancer cell viability due to tailored CUR release from CUR-NPs. In conclusion, jackfruit gum-genipin-based CUR-NPs offered high entrapment efficiency, tailored releases of CUR, good mucoadhesive property and improved anticancer activity.

Keywords: jackfruit gum, genipin, ionotropic gelation, curcumin, nanoparticles, sustained release

INTRODUCTION

Cancer poses a substantial challenge in the realm of healthcare due to its hallmark of abnormal and unregulated cellular proliferation. This malignancy stands as a global health crisis of utmost severity, with its impact spanning across the entire world.^{1,2} Projections from the World Health Organization (WHO) indicate a disconcerting trend, forecasting an escalation in cancer-related mortalities to reach 12 million cases by 2030. In parallel, the incidence of cancer diagnoses is anticipated to surge, with a global estimate of 24 million cases by the year 2035.³ Colorectal cancer ranks as the third most common and second deadliest cancer worldwide. In 2020, it accounted for 1.9 million reported cases and 0.9 million fatalities, with projections suggesting a rise to 3.2 million cases by 2040.⁴ Surgery is the primary method used to treat colorectal cancer,⁵ but unfortunately, over half of patients experience recurrence and metastasis after resection.^{6,7} Recent data indicates that chemotherapy and radiation are the most frequently employed cancer treatment options. Among chemotherapy agents,

irinotecan, oxaliplatin, and capecitabine have shown promise in clinical trials for colorectal cancer treatment,⁵ despite exhibiting drug resistance and causing significant harm to normal tissues.^{8,9} However, in spite of their usefulness, both chemotherapy and radiation therapies have substantial drawbacks that need to be addressed before they can be considered successful cancer treatment methods.¹⁰ These limitations include non-selectivity, dose-dependent toxicity, resistance development, and others.^{2,11,12} Consequently, there is a growing urgency to explore natural products, particularly phytoconstituents, renowned for their anticancer attributes, including their capacity to trigger apoptosis and inhibit tumor growth, while sparing healthy cells. Such natural substances, which are derived from food or serve as food ingredients and confer health or medical advantages, fall under the category known as nutraceuticals.¹³ Therefore, we intend to use a natural anticancer phytoconstituent for the design of an anticancer dosage form.

Curcumin (CUR) is a bioactive compound derived from the turmeric plant (*Curcuma longa* L.), demonstrating multifaceted properties, including antioxidant, antimicrobial, and antitumor effects across various cancer cell lines.¹⁴ While it may not match the potency of some cytotoxic agents, it boasts a commendable safety profile in humans even at relatively high doses, rendering it an attractive candidate for incorporation into chemotherapeutic drug delivery strategies.¹⁵ Addressing its limitations, CUR can be complexed with appropriate substances, such as cyclodextrin, phospholipids, and piperine, effectively integrated into nanoparticles. Scientific literature underscores CUR's effectiveness against an array of cancer types, encompassing prostate cancer, bone cancer, lung cancer, head and neck cancer, breast cancer, and gastrointestinal cancer.¹⁶ Despite its remarkable properties, the widespread utilization of CUR in cancer treatment is hindered by its inherent poor aqueous solubility. Additionally, CUR encounters challenges related to low gastrointestinal absorption, limited bioavailability, and rapid metabolism.^{14,17} In the realm of drug delivery, micro- and nanoparticles have garnered substantial interest, primarily for their ability to facilitate sustained drug release to maintain therapeutic dosage levels as required.^{18,19} In this context, the utilization of CUR-loaded polymeric nanoparticles (CUR-NPs) emerges as a promising and viable solution for the effective delivery of CUR in colorectal cancer treatment.

The preference for natural carbohydrates, such as gum, is widely reported in biomedical applications.²⁰ It offers several advantages in drug delivery systems, including biocompatibility, good swelling and mucoadhesion potential, biodegradability, surface tunability, *etc.*²¹ The interest in jackfruit-based polymeric materials has been noted in biomedical research.²⁰ Here, the use of jackfruit mucilage in the design of dosage forms offers superior merits that can be used for the design of advanced drug delivery systems.²² The design of polymeric dosage by using suitable crosslinkers offers the modified release of therapeutic agents.²¹ In this context, the introduction of crosslinkers plays a pivotal role in enhancing the mechanical properties of polymers, while regulating the release dynamics of active agents.²³ Natural crosslinking agents are favored over synthetic counterparts in the realm of drug delivery due to their non-toxic and biocompatible attributes.²⁴ Genipin, a naturally derived

crosslinker, is harnessed to enhance the control over the release behavior. It is obtained from geniposide, an extract derived from gardenia fruits.²⁵ Furthermore, alongside these natural agents, montmorillonite (MMT) is widely preferred in pharmaceutical formulations as a non-toxic reinforcing agent. Not only does MMT aid in governing the release of therapeutic agents, but it also possesses the capability to adsorb dietary toxins.²³ To the best of our knowledge, there are no reports available in the literature on jackfruit gum based nanoformulations for drug delivery in cancer management. Therefore, jackfruit gum with genipin and MMT were investigated in this study to design an advanced crosslinker polymeric nanocarrier for delivery of CUR in colorectal cancer.

This work aimed to design jackfruit gum-based genipin crosslinked nanoparticles (CUR-NPs) for modified release of CUR, using the ionotropic gelation technique, and their evaluation against colorectal cancer cell lines. In brief, we utilized a 3² (three-level, two-factor) response surface methodology to investigate the impact of independent variables, namely the ratio of jackfruit gum to MMT (X1) and the concentration of genipin (X2), on dependent variables, including % encapsulation efficiency (EE, Y1) and % drug release (DR, Y2). Here, the physicochemical properties of the developed CUR were studied using Fourier transform-infrared (FTIR) spectroscopy and X-ray powder diffraction (XRPD), and by swelling behavior, mucoadhesiveness and *in-vitro* drug release studies. The blending mixture of jackfruit gum with MMT improved drug encapsulation and the stability of the formulations. At last, the anticancer activity against the HCT116 human colorectal cancer cells confirmed the anticancer potential of designed jackfruit gum-based CUR-NPs. In the future, the use of jackfruit gum for designing nanosized dosage forms may open a new platform for the delivery of anticancer phytoconstituents in colorectal cancer, as well as other types of cancer.

EXPERIMENTAL

Materials

Jackfruit gum was purchased from South Fine Foods Pvt. Ltd., Sira, Tumkur, Karnataka. Montmorillonite K-10 (MMT) and CUR were purchased from Sigma-Aldrich. Genipin was acquired from Challenge Bioproducts Co., Taiwan. All the

chemicals used in this research were of analytical grade.

Methods

Preparation of jackfruit gum-based CUR nanoparticles (CUR-NPs)

In this step, the jackfruit gum and genipin were ionically crosslinked to create nanoparticles (NPs) using a suitable natural crosslinker (genipin). In brief, a 1% solution of jackfruit gum was prepared using double distilled water. Concurrently, montmorillonite (MMT) was immersed in 50 mL of distilled water for 24 h, vigorously agitated using a mechanical stirrer for two days, and subsequently subjected to 30 min of sonication. The well-dispersed MMT was then introduced into a 50 mL solution of 1% jackfruit gum. Additionally, 0.01 g of CUR was dissolved in a 60%

ethanol-water mixture and incorporated into the aforementioned solution. A 1% (w/v) genipin solution was prepared in water. The formation of CUR-loaded nanoparticles (CUR-NPs) involved the addition of 15 mL of the genipin solution to a 100 mL MMT dispersion, with continuous stirring at room temperature for 30 min. During this process, the genipin solution was gradually introduced, and the temperature was elevated to 45 °C to facilitate the crosslinking of the nanoparticles. This reaction continued for approximately 2 h. Subsequently, the mixture underwent cold centrifugation at 10,000 rpm for 30 min, and the resultant nanoparticles were washed thrice with deionized water prior to undergoing freeze-drying.²⁶ Likewise, a series of samples were prepared by varying the quantities of MMT clay and genipin, as outlined in Table 1.

Table 1
Formulations of CUR-NPs

Experimental run	Independent variables		Dependent variables	
	Jackfruit gum: MMTe ratio (X ₁)	% Genipin (X ₂)	% EE (Y ₁)	% Drug release (Y ₂)
F1	0	-1	64.15	88.02
F2	1	-1	66.6	98.74
F3	-1	0	73.69	97.69
F4	0	0	79.02	98.2
F5	1	0	83.99	98.36
F6	0	0	77.18	98.15
F7	-1	1	68.78	98.58
F8	0	0	76.25	94.336
F9	0	0	77.69	97.65
F10	0	1	66.23	91.14
F11	1	1	81.79	90.65
F12	0	0	78.54	95.15
F13	-1	-1	70.2	91.33
Coded levels				
Independent variable	Low level (-1)	Medium level (0)	High level (+1)	
X ₁ = Jackfruit gum to MMT ratio	1	2	3	
X ₂ = % genipin	0.2	0.4	0.6	

Experimental design for optimization

The experimental study utilized Design-Expert software from Stat-Ease Inc., Minneapolis. To optimize the process and determine the impact of independent variables on responses, a 3² (three-level, two-factor) response surface methodology was preferred.²⁷ In short, the independent variables chosen were the jackfruit gum to MMT ratio (X₁) and the concentration of genipin (X₂ %), each of which was varied at three levels: low (-1), medium (0), and high (+1). The dependent factors selected were % EE (entrapment efficiency, Y₁) and % drug release (Y₂). The statistical design for the specified dependent

factors and independent variables is provided in Table 1. For optimization, the influence of independent variables (X₁, X₂) on dependent variables (Y₁, Y₂) was modeled using the following equation:

$$Y = \beta_0 + \beta_1 x_1 + \beta_2 x_2 + \beta_3 x_1 x_2 + \beta_4 x_1^2 + \beta_5 x_2^2 \quad (1)$$

where Y is the response, β_0 is the intercept, β_1 to β_5 are regression coefficients, X_1 and X_2 are individual effects, $X_1 X_2$ is the interaction effect, X_1^2 and X_2^2 are the quadratic effects. The significance of the model was evaluated at a significance level of $P < 0.05$ using one-way ANOVA.

Characterization

Spectroscopical characterization

Fourier-transform infrared spectroscopy (FTIR) was used to investigate the potential interactions between CUR and the excipients. In brief, FTIR spectra of pure CUR, jackfruit gum, and CUR-NPs were recorded across the wavelength range of 4000 to 400 cm^{-1} . The analysis of these spectra allowed us to assess the compatibility of the ingredients within the formulations. Samples were prepared in a 1:10 ratio using potassium bromide (KBr) and were scanned with a resolution of 1.0 cm^{-1} against a blank KBr disc. The particle size of CUR-NPs was analyzed using a particle size analyzer (Nanoplus 3). Subsequently, the zeta potential was determined by diluting the samples with tenfold the amount of water, utilizing a Malvern Zetasizer (Model: ZS 200). The physical state of CUR, jackfruit gum, and CUR-NP was characterized using a differential scanning calorimeter (DSC). Here, 2–3 mg of sample was encapsulated in aluminum pans with lids. The sample was then subjected to a heating rate of 10 $^{\circ}\text{C}/\text{min}$, ranging from 20 to 200 $^{\circ}\text{C}$, within a DSC pan. Throughout the experiment, a nitrogen gas flow rate of 80 mL/min was maintained. Using the provided software, various thermal characteristics of the samples were determined, including their melting points, as well as the enthalpies associated with endothermic and exothermic reactions. X-ray powder diffraction (XRPD) was employed to assess the crystal state of the formulations. Here, a D₈ Advance diffractometer from Bruker, Germany, equipped with Cu/K α radiation ($\lambda = 1.54 \text{ \AA}$) in the scanning range of 5–80 $^{\circ}$ (2 θ) with a step size of 0.05, was used to analyze the selected materials.

Entrapment efficiency (EE)

The concentration of CUR in jackfruit gum-based CUR-NPs was determined utilizing a UV-Vis spectrophotometer (Hitachi U2900).²⁸ Roughly 50 mg of CUR-loaded nanoparticles (CUR-NPs), equivalent in weight, were introduced into a 100 mL volumetric flask. Subsequently, 100 mL of phosphate buffer (PBS) with a pH of 6.8 was added, and the mixture was agitated for 24 h at a temperature of 37 \pm 2 $^{\circ}\text{C}$, employing an orbital shaking incubator (Remi, India). The resulting solution was then passed through Whatman filter paper, and the ultimate filtrate was subjected to analysis at a wavelength of 209 nm, using a UV-Vis spectrophotometer. Finally, the percentage encapsulation efficiency (% EE) was reported using the following equation:

$$\text{EE (\%)} = \frac{\text{Weight of drug determined (mg)}}{\text{Weight of drug added (mg)}} \times 100 \quad (2)$$

Evaluation of swelling behavior

The swelling characteristics of an optimized batch of CUR-NPs were assessed in distinct environments, including pH 1.2 HCl buffer and pH 7.4 phosphate buffer. These investigations were carried out under

controlled conditions, involving stirring at 50 rpm and a temperature of 37 \pm 10 $^{\circ}\text{C}$. The experiments were executed utilizing a paddle-type dissolution test apparatus. In each trial, 100 mg of CUR-NPs were introduced into the dissolution apparatus vessel, which contained 500 mL of the corresponding dissolution medium. At predetermined intervals, the swollen CUR-NPs were retrieved and their weights were recorded. This procedure was repeated until a consistent weight was attained. The swelling index was calculated employing the following formula:

$$\text{Swelling index (\%)} = \frac{\text{Weight of beads after swelling} - \text{Dry weight of beads}}{\text{Dry weight of beads}} \times 100 \quad (3)$$

Ex vivo mucoadhesion study

The mucoadhesive properties of the optimized batch of CUR-NPs were assessed using the *ex vivo* wash-off method.²⁹ A freshly excised segment of goat intestinal mucosa, measuring 2 \times 2 cm, was securely attached to a glass slide, measuring 7.5 \times 2.5 cm. Approximately 50 mg of CUR-NPs were affixed to this slide, which was subsequently suspended within a groove of a disintegration tester. The experiments were carried out in distinct vessels, each containing 900 mL of pH 1.2 HCl buffer and phosphate buffer at pH 7.4, respectively. The tissue sample, along with the glass slide, underwent a repetitive up-and-down motion within the laboratory disintegration tester.

In vitro drug release

Dissolution studies of jackfruit gum-based CUR-NPs were conducted using a USP paddle-type dissolution tester. In a nutshell, dissolution media consisting of 0.1 N HCl (pH 1.2) and phosphate buffer (PBS) at pH 7.4 were employed. Throughout the study, stirring was consistently maintained at a rate of 50 rpm, and the temperature was rigorously controlled at 37 \pm 0.2 $^{\circ}\text{C}$. To execute these studies, an equivalent weight of 50 mg of CUR-NPs was placed within a pre-treated dialysis bag, which was subsequently introduced into the dissolution vessels having 900 mL of 0.1 N HCl for 2 h. Following this period, the dissolution medium was transitioned to phosphate buffer at pH 7.4. Samples from vessels were collected using a syringe at predefined time intervals, such as 2, 4, 6, 8, 10, and 12 h. The collected samples were then subjected to a filtration process using Whatman filter paper. To ensure a sink condition during the dissolution process, 5 mL of fresh dissolution medium was introduced after every sample collection (5 mL). The filtrate was subjected to analysis using a UV-Vis spectrophotometer at a wavelength of 426 nm. To elucidate the mechanism of release and release rate kinetics for the dosage form, the acquired data were fitted to various models, encompassing the zero order, first order, Higuchi matrix, Peppas, and Hixson Crowell models. The selection of the most appropriate model was determined by comparing the R² values obtained.

Cell line study

In our research, we employed the HCT116 human colorectal cancer cells and followed standard techniques for cell culture and maintenance. In brief, the cells were cultivated in a sterile incubator at 37 °C with 5% CO₂ (carbon dioxide). They were allowed to proliferate in growth media until reaching 80-90% confluence. Following this, the media was removed, and the cells were rinsed with sterile PBS. Subsequently, the cells were trypsinized and transferred to a fresh flask with new growth media. Cell viability was assessed using an MTT assay, where 4×10^4 HCT116 human colorectal cancer cells were seeded in a 24-well plate and transfected with 10 µg of CUR-NPs dispersed in the medium. Transfections were conducted at 24, 48, and 72 h time points. Cells were washed with phosphate-buffered saline (PBS) every 24 h, and 500 µL of 10% MTT dye (MTT: 3-(4,5-dimethylthiazol-2-yl)-2,5-diphenyltetrazolium bromide) in Dulbecco-modified Eagle's medium (DMEM) was added to each well. The cells were then incubated for 3 h. Subsequently, the MTT-containing media were aspirated, and dimethyl sulfoxide (DMSO) was added. A microplate reader (Fluostar Omega Multi-Mode Microplate Reader) was used to measure the absorbance at 570 nm.

RESULTS AND DISCUSSION

Optimization

To assess the effects of independent variables (X_1 , X_2) on dependent variables (Y_1 , Y_2), a 3²-response surface methodology was employed. In essence, two-dimensional (2D) plots (Fig. 1A, and B) and three-dimensional (3D) counterplots (Fig. 1C, and D) were used to analyze the influence of independent variables. Herein, the 3D response surface graphs proved to be particularly valuable in discerning the primary and interaction effects of the independent variables. In this study, the independent variables, including the jackfruit gum to MMT ratio (X_1) and the concentration of the genipin solution (X_2), show their impact on dependent variables – % EE and % drug release. As an output, the 2D and 3D plots for % EE revealed that % EE increased with higher values of jackfruit gum to MMT ratio (X_1). Here, the concentration of genipin solution (X_2) shows the rise in concentration resulted in a reduction in % EE of CUR in NPs.

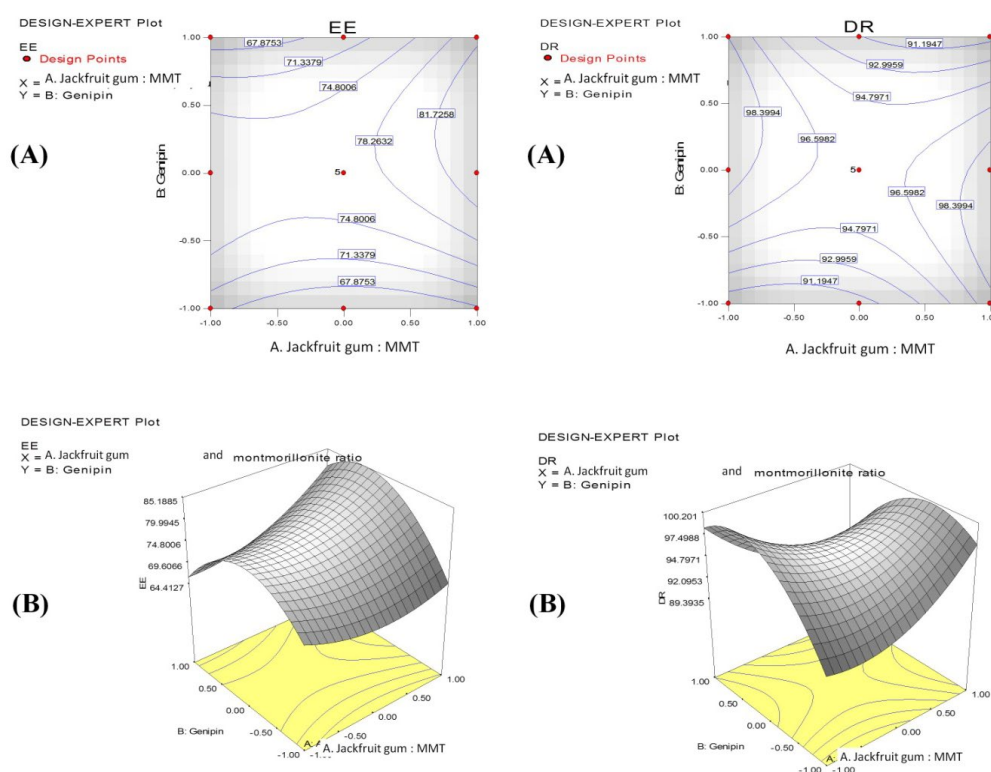


Figure 1: 2D contour plot for (A) % EE and (B) drug release (DR) from CUR-NPs; 3D response surface plot for (C) % EE and (D) drug release from CUR-NPs

Table 2
Summary of results of regression analysis for responses Y₁ and Y₂

Source	Std. Dev.	R-Squared	Adj. R-Squared	Predicted R-Squared	PRESS*	Remarks
Response EE						
Linear	6.181156	0.218173	0.061808	- 0.50851	737.1863	
2 FI	5.898153	0.359313	0.145751	- 0.42925	698.4549	
Quadratic	2.512165	0.909601	0.84503	0.311745	336.3398	Suggested
Cubic	2.282373	0.946702	0.872084	- 4.06292	2474.174	
Response drug release						
Linear	4.091807	0.00517	- 0.1938	- 1.06533	347.5934	
2 FI	3.473711	0.35472	0.139627	- 0.13411	190.8688	
Quadratic	2.010467	0.831884	0.7118	0.186366	136.9337	Suggested
Cubic	2.183041	0.858417	0.6602	- 6.42148	1249.028	

*Predicted residual error sum of squares

Conversely, DR increased with an increase in both the jackfruit gum to MMT ratio (X₁) and the genipin concentration (X₂). In all 13 experimental runs, % EE ranged from 64.15 ± 1.45% to 83.99 ± 1.40%, and % drug release ranged from 88.02 ± 0.87% to 98.74 ± 0.96%, as detailed in Table 1. To establish the mathematical relationships between dependent and independent variables, polynomial equations and counterplots were employed. For both Y₁ and Y₂ responses, the quadratic model resulted in correlation coefficient (R²) values of 0.9096 and 0.8318, respectively, indicating a good fit (as shown in Table 2).

The equations for EE (Y₁) and DR (Y₂) responses are as follows:

$$Y_1 = +76.97 + 3.28x_1 + 2.64x_2 + 3.78x_1^2 - 9.87x_2^2 + 4.15x_1x_2 \quad (3)$$

$$Y_2 = +96.16 + 0.025x_1 + 0.38x_2 + 3.22x_1^2 - 5.23x_2^2 - 3.83x_1x_2 \quad (4)$$

In the equations above, positive values as well as negative values indicate synergistic and antagonistic effects, correspondingly. The ANOVA results for Y₁ and Y₂ responses are presented in Table 3. For EE (Y₁), the quadratic equation suggests that it is influenced by the independent variables X₁, X₂, X₁², X₂², and X₁X₂. Similarly, in the case of the drug release (Y₂) response, it also follows a quadratic equation, influenced by the independent factors X₁, X₂, X₁², X₂², and X₁X₂. The consequence of these independent variables on % EE and % CUR release were found to be statistically significant at P < 0.05. Importantly, both models were significant, with F values of 14.08 and 0.012 at P < 0.05.

Table 3
ANOVA of models for Y₁ and Y₂

Source	Sum of squares	DF	Mean square	F Value	Prob > F	Remarks
Response Y ₁						
Model	444.5078	5	88.90156	14.08682	0.0015	
X ₁	64.74735	1	64.74735	10.25948	0.0150	
X ₂	41.87042	1	41.87042	6.63454	0.0367	
X ₁ ²	39.51722	1	39.51722	6.261666	0.0409	Significant
X ₂ ²	268.9152	1	268.9152	42.61072	0.0003	
X ₁ X ₂	68.97303	1	68.97303	10.92906	0.0130	
Response Y ₂						
Model	140.0052	5	28.00104	6.92756	0.0123	
X ₁	0.00375	1	0.00375	0.000928	0.9766	
X ₂	0.8664	1	0.8664	0.214351	0.6574	
X ₁ ²	28.6163	1	28.6163	7.079777	0.0324	Significant
X ₂ ²	75.43457	1	75.43457	18.66279	0.0035	
X ₁ X ₂	58.8289	1	58.8289	14.55449	0.0066	

Table 4 furnishes diagnostic statistics pertaining to a range of response variables, encompassing actual, forecasted, and residual values. The evaluation of prediction errors was conducted by juxtaposing the experimental values

against the anticipated values. The minimal disparities observed between the actual and forecasted values signify that the model exhibited a robust alignment with the dataset.

Table 4
Diagnostics statistics for various response variables

Standard order	Actual value	Predicted value	Residual	Standard order	Actual value	Predicted value	Residual
Response Y ₁				Response Y ₂			
F1	70.2	69.1117	1.088305	F1	91.33	89.90962	1.420379
F2	64.15	64.46161	-0.31161	F2	88.02	90.55076	-2.53076
F3	66.6	67.3767	-0.7767	F3	98.74	97.62962	1.110379
F4	73.69	77.46828	-3.77828	F4	97.69	99.35076	-1.66076
F5	76.25	76.97069	-0.72069	F5	94.336	96.1569	-1.8209
F6	83.99	84.03828	-0.04828	F6	98.36	99.40076	-1.04076
F7	68.78	66.09003	2.689971	F7	98.58	98.33962	0.240379
F8	66.23	69.74494	-3.51494	F8	91.14	91.31076	-0.17076
F9	81.79	80.96503	0.824971	F9	90.65	90.71962	-0.06962
F10	77.69	76.97069	0.71931	F10	97.65	96.1569	1.493103
F11	77.18	76.97069	0.20931	F11	98.15	96.1569	1.993103
F12	78.54	76.97069	1.56931	F12	95.15	96.1569	-1.0069
F13	79.02	76.97069	2.04931	F13	98.2	96.1569	2.043103

% EE

In this analysis, a 3D counter-plot predicts the effects of the ratio of jackfruit gum to MMT and the concentration of genipin on the % EE factor. In the 13 experiments conducted, EE ranged from 64.15% to 83.99%. Notably, at a genipin concentration of 0.2% and a 1:1 ratio of jackfruit gum to MMT, the formulation exhibited an impressive $83.99 \pm 1.23\%$ EE. Hence, we conclude that EE tends to increase with a lower genipin concentration, while maintaining the same proportion of jackfruit gum to MMT ratio. Here, the rise in the concentration of crosslinkers may reduce the extra space in polymeric networks that reduce the EE of polymeric dosage forms.²¹

In vitro drug release

The *in-vitro* drug release profile is a valuable tool for understanding how the prepared CUR-NPs release the drug within the gastrointestinal tract. Herein, the release profile of the optimized CUR-NPs falls within the range of $88.02 \pm 0.87\%$ to $98.74 \pm 0.96\%$ over a 12 h duration. It is worth

noting that optimized CUR-NPs exhibit sustained release behavior for up to 12 h, as depicted in Figure 2. Here, the release of CUR from a physical mixture of jackfruit gum (in the absence of crosslinker) shows a $97.23 \pm 0.62\%$ drug release within 12 h. Here, the presence of the crosslinker in the nanoparticles offers a barrier for tailored release of CUR from CUR-NPs. Also, the lowest concentration of genipin with a lower ratio of concentration of jackfruit gum and MMT shows a reduction in drug release. The rise in concentration of genipin with a rise in the ratio of the concentration of jackfruit gum and MMT provides a lower release of CUR in CUR-NPs. To determine the CUR release kinetics, the release data were fitted to different kinetic models. More details regarding the medication release mechanism for all batches are provided in Table 5. It shows the highest linearity in regression coefficient (R^2 : 0.9882) for the Korsmeyer-Peppas model, indicating a significant fit for the *in vitro* drug release.

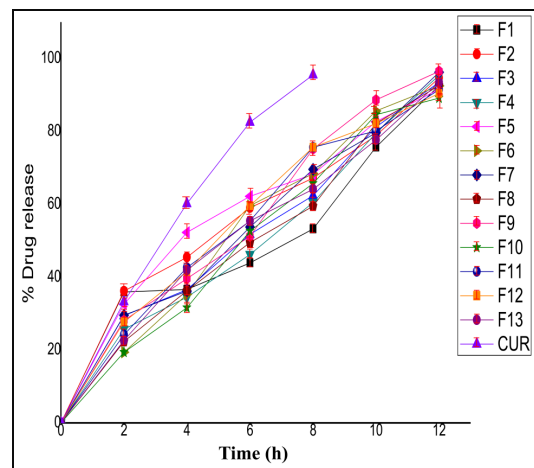


Figure 2: *In vitro* dissolution profiles of CUR-NPs

Table 5
In vitro release kinetic for CUR-NPs

Kinetic model	F1	F2	F3	F4	F5	F6	F7	F8	F9	F10	F11	F12	F13
Zero order model	0.9013	0.8869	0.9637	0.9821	0.8616	0.9765	0.9655	0.9848	0.9848	0.9866	0.9484	0.9304	0.9672
First order model	0.941	0.8951	0.8951	0.8951	0.8951	0.8951	0.9	0.8857	0.961	0.961	0.958	0.9643	0.9636
Higuchi model	0.8205	0.9651	0.9519	0.9408	0.987	0.9885	0.9624	0.9656	0.9656	0.982	0.9891	0.9889	0.9876
Korsmeyer-Peppas model	0.787	0.9698	0.9551	0.9586	0.9882	0.9884	0.9579	0.9886	0.9656	0.9897	0.9922	0.9908	0.9938

FTIR analysis

Figure 3 displays the FTIR spectra of pure CUR, jackfruit gum, and CUR-NPs. The FTIR of CUR exhibits characteristic peaks at 3241 cm^{-1} (O-H stretching vibrations), 1694.14 cm^{-1} (indicating C=O in the ring), 1452.18 cm^{-1} (C=C carbonyl stretching vibrations), 1257.44 cm^{-1} (C-O stretching vibrations), and 1108 cm^{-1} , 1390 cm^{-1} (C-O-C stretching vibrations). The FTIR spectrum of jackfruit gum reveals characteristic peaks at 3441 cm^{-1} (O-H stretching), 2975 cm^{-1} (C-H stretching), 1704 cm^{-1} (C=O stretching vibrations), 1644 cm^{-1} (C=C stretching vibrations), 1456 cm^{-1} (O-H bending vibrations), and 1381 cm^{-1} (C-O stretching vibrations). In the CUR-NPs spectrum, various characteristic peaks of both CUR and jackfruit gum were observed. Also, these peaks did not display any significant deviation, suggesting an absence of interaction between the components. Overall, the FTIR analysis confirmed the presence of CUR in the prepared jackfruit gum-based CUR-NPs.

Particle size distribution and zeta potential

Particle size and polydispersity index (PDI) of optimized CUR-NP (Fig. 4A) formulations were obtained to be 120.32 nm , and 0.23 , respectively. Here, the PDI confirmed the uniform dispersion of CUR-NPs in a solvent system. Also, particle size analysis confirmed the formation of nanosized CUR-NPs using jackfruit gum and

genipin. The zeta potential of the CUR-NPs (optimized batch) was found to be -17.34 mV , suggesting good stability when compared to pure CUR (Fig. 4B). Overall, the particle size and zeta potential analysis ensured the formation of stable, uniformly distributed nanosized CUR-NPs from the jackfruit gum and genipin.

DSC analysis

Thermal analysis was conducted to investigate interactions among CUR, jackfruit gum, and CUR-NPs. In short, the thermograms of pure CUR, jackfruit gum, and CUR-NPs are presented in Figure 5. Herein, a sharp endothermic peak at $187.4\text{ }^{\circ}\text{C}$ was obtained in the thermogram of pure CUR, corresponding to the melting point of pure CUR. Jackfruit gum exhibited a more or less endothermic peak in the range of $40\text{ }^{\circ}\text{C}$ to $60\text{ }^{\circ}\text{C}$, likely due to hydration. Also, there is no peak observed that might be caused by the amorphous nature of the gum. At last, the thermogram of CUR-NPs shows the endothermic peak at $187.2\text{ }^{\circ}\text{C}$, confirming the presence of CUR in the jackfruit gum-based crosslinked polymeric matrix. Importantly, a reduction in the peak intensity of CUR was observed in the endothermic peaks of CUR-NPs. Possibly, it is because of the incorporation of CUR in the crosslinker jackfruit gum. Also, these polymeric networks help to reduce the crystalline nature of CUR.

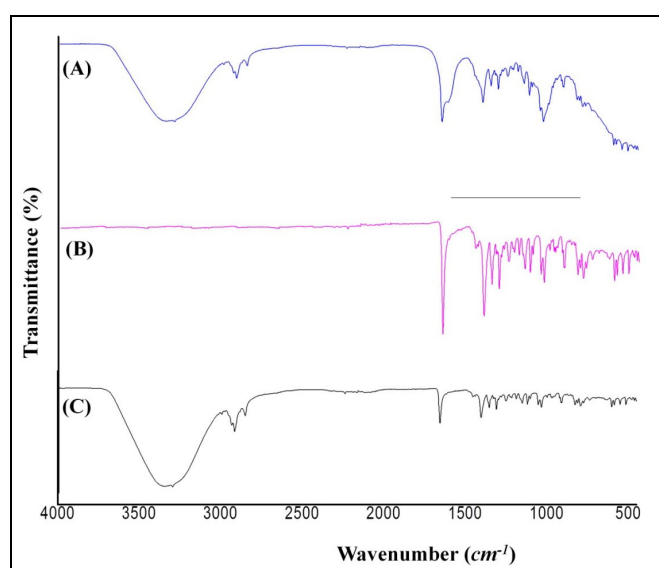


Figure 3: FTIR spectra of (A) jackfruit gum, (B) CUR, and (C) CUR-NPs

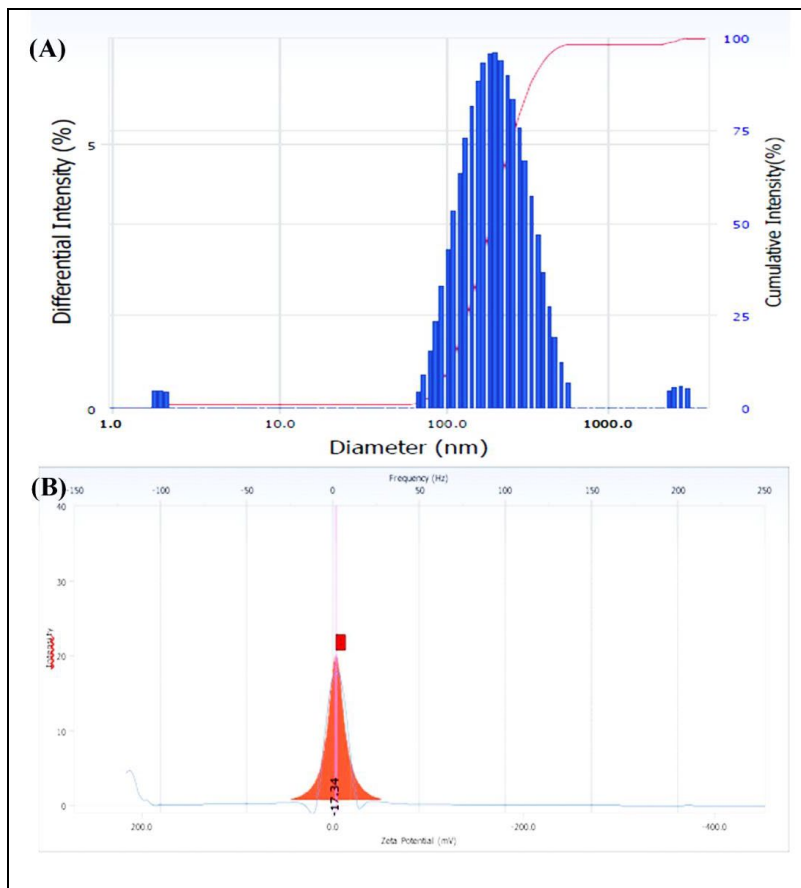


Figure 4: (A) Particle size and (B) zeta potential analysis of CUR-NPs

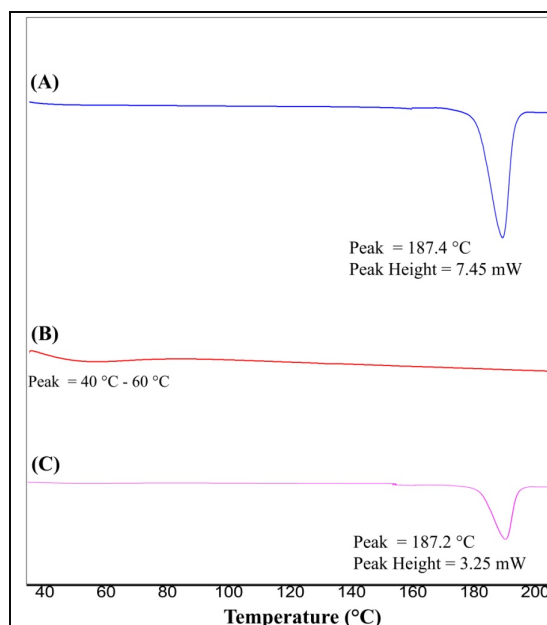


Figure 5: Thermograms of (A) CUR, (B) jackfruit gum, and (C) CUR-NPs

XRPD analysis

The diffractogram of bare CUR in Figure 6A displays sharp diffraction peaks at 2θ angles of 9.02° , 13.94° , 17.42° , 19.93° , 22.18° , and 26.65° , indicating its crystalline form. However, the

intensity of these peaks was notably reduced in the diffractogram of the prepared CUR-NPs (Fig. 6B), suggesting an amorphous form. This indicates a decline in the crystallinity of the CUR, as evidenced by the diminished peak intensity.

Importantly, it is because of the insertion of CUR in genipin crosslinked jackfruit gum-mediated polymeric nanoparticles.

Swelling behavior

Figure 7 illustrates the swelling behavior of the CUR-NPs formulation (optimized batch). The prepared CUR-NPs exhibit pH-dependent swelling. Notably, the swelling index of CUR-NPs in phosphate buffer at pH 7.4 (alkaline

media) is lower than the swelling index in 0.1 N HCl (acidic media). This variation in the swelling behavior of the optimized CUR-NPs can be attributed to the inherent swelling ability of jackfruit gum when exposed to liquid media. Here, less swelling in pH 7.4 buffer media plays a key role in the tailored release of CUR from CUR-NPs that is meritorious for the treatment of colorectal cancer.

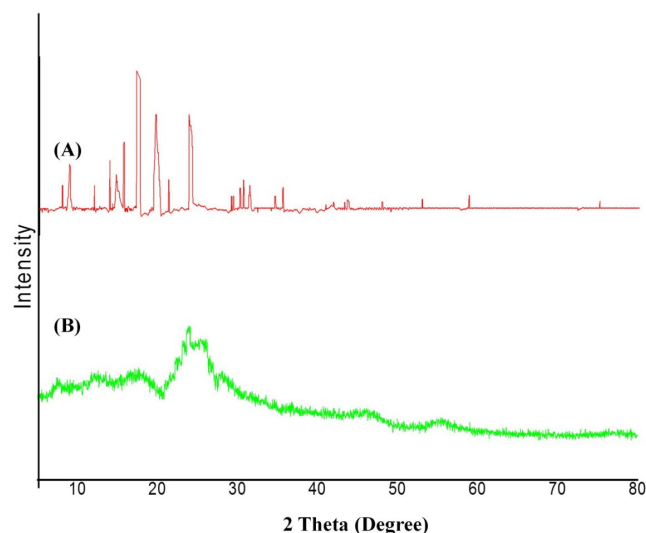


Figure 6: Diffractograms of (A) CUR and (B) CUR-NPs

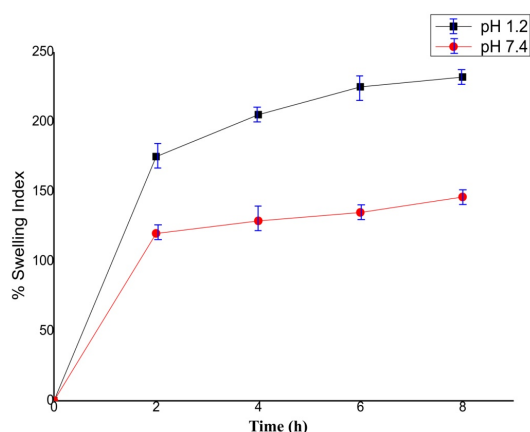


Figure 7: Swelling behavior of optimized CUR-NPs formulations in 0.1 N HCl (pH 1.2), and phosphate buffer (pH 7.4)

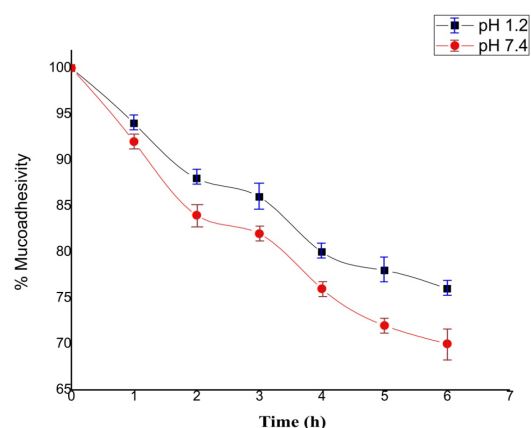


Figure 8: Mucoadhesive behavior of optimized CUR-NPs in 0.1 N HCl (pH 1.2), and phosphate buffer (pH 7.4)

Ex vivo mucoadhesion testing

In Figure 8, we depict the outcomes of the *ex vivo* wash-off experiment with the optimized CUR-NPs, employing goat intestinal mucosa, under two distinct conditions: acidic gastric (0.1 N HCl, pH 1.2) and alkaline intestinal (phosphate buffer, pH 7.4). Notably, the results reveal a heightened level of mucoadhesion in the acidic

environment of 0.1 N HCl, when compared to the phosphate buffer at pH 7.4. The mucoadhesiveness of the optimized CUR-NPs was approximately $76 \pm 1.45\%$ over 6 h in 0.1 N HCl and $70 \pm 1.30\%$ over 6 h in phosphate buffer at pH 7.4. This enhanced mucoadhesive property, attributed to jackfruit gum, extends the residence time and contact with the absorptive membrane

for CUR, potentially leading to increased oral bioavailability and improved therapeutic effectiveness.

Cell viability analysis

To assess cell viability, the MTT assay was employed. HCT116 human colorectal cancer cells were transfected with 10 μg of CUR-NPs, while control cells were transfected with CUR-NPs and 10 μg of pure CUR. Transfection durations included 24, 48, and 72 h. After 24 h of treatment with CUR-NPs, the cell viability of HCT116 human colorectal cancer cells decreased to $73.45 \pm 2.01\%$. The release of drugs from the nanoparticles led to a reduction in cell viability, potentially causing cell death (Fig. 9). It is important to note that pure CUR also exhibited

cytotoxic effects on the cells. The cell viability decreased by $45.22 \pm 1.22\%$ for pure CUR and $42.09 \pm 0.96\%$ for CUR-NPs after 72 h of exposure. Here, the acidic pH of cancerous cells helps to tailor the release of CUR from the CUR-NPs. Possibly, it is because of less protonation of jackfruit gum into acidic pH the cancer cells. Overall, the designed CUR-NPs offer good anticancer potential against the colorectal cancer cell lines. In the case of placebo NPs, there is no decline in cell viability of HCT116 cell lines. Hence, it confirmed that the CUR plays a key role in anticancer activity. In the future, there is a need to perform cellular bioimaging and preclinical studies to ensure the potential of designed CUR-NPs in the management of colorectal cancers.

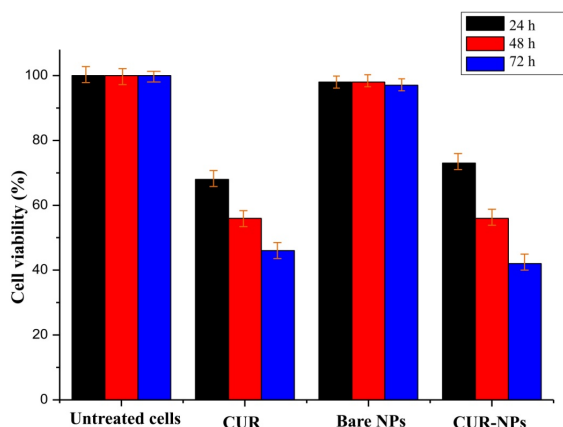


Figure 9: Cell viability analysis of CUR-NPs using HCT116 human colorectal cancer cells

CONCLUSION

In the present work, jackfruit gum-based modified release CUR-NPs were designed and prepared using the ionotropic-gelation method for improved anticancer activity. In brief, a 3^2 response surface methodology confirmed the effects of independent factors, such as the jackfruit gum to MMT ratio (X_1) and genipin concentration (X_2), on dependent variables, including % EE (Y_1) and drug release (Y_2). Importantly, the drug release ranged from $88.02 \pm 0.87\%$ to $98.74 \pm 0.96\%$ over 12 h, while the percentage of EE varied from $64.15 \pm 1.45\%$ to $83.99 \pm 1.40\%$. Also, the optimized CUR-NPs displayed favorable mucoadhesive properties. The thermogram indicated the absence of interaction between CUR and jackfruit gum. The diffractogram suggested the amorphous nature of the CUR-NPs. The swelling behavior of the optimized CUR-NPs could be attributed to the

propensity of jackfruit gum to swell in liquid environments. These optimized CUR-NPs exhibited prolonged residence time and improved interaction with the absorptive membrane of CUR, owing to the mucoadhesive characteristics of jackfruit gum. Furthermore, the cell viability of HCT116 human colorectal cancer cells decreased when treated with CUR-NPs. In conclusion, the presence of jackfruit gum in the design of CUR-NPs demonstrates good mucoadhesion ability, high drug entrapment, tailored release of CUR, and improved cancer cell toxicity. Therefore, in the future, jackfruit gum can be used as an excellent alternative for the delivery of anticancer drug molecules in the management of colorectal cancer.

ACKNOWLEDGMENTS: The authors would like to express their gratitude to Dr. S. J. Surana, the Principal of R. C. Patel Institute of

Pharmaceutical Education and Research, Shirpur, for providing the necessary facilities to conduct this research.

REFERENCES

- ¹ J. Pantwalawalkar, P. Mhetar, S. Nangare, R. Mali, A. Ghule *et al.*, *ACS Biomater. Sci. Eng.*, **9**, 4497 (2023), <https://doi.org/10.1021/acsbomaterials.3c00507>
- ² J. Pantwalawalkar, S. Chandankar, R. Tade, Z. Khan, M. Shaikh *et al.*, *Adv. Nat. Sci.: Nanosci. Nanotechnol.*, **13**, 013001 (2022), <https://doi.org/10.1088/2043-6262/ac5e35>
- ³ M. Gültekin, P. Ramirez, N. Broutet and R. Hutubessy, *Int. J. Gynecol. Cancer.*, **30**, 426 (2020), <https://doi.org/10.1136/ijgc-2020-001285>
- ⁴ Y. Xi and P. Xu, *Transl. Oncol.*, **14**, 101174 (2021), <https://doi.org/10.1016/j.tranon.2021.101174>
- ⁵ G. Ramírez-Rico, M. E. Drago-Serrano, N. León-Sicairos and M. de la Garza, *Front. Pharmacol.*, **13**, 421 (2022), <https://doi.org/10.3389/fphar.2022.855852>
- ⁶ X. Gu, Y. Wei, Q. Fan, H. Sun, R. Cheng *et al.*, *J. Control. Release*, **301**, 110 (2019), <https://doi.org/10.1016/j.jconrel.2019.03.005>
- ⁷ C. J. Punt, M. Koopman and L. Vermeulen, *Nat. Rev. Clin. Oncol.*, **214**, 235 (2017), <https://doi.org/10.1038/nrclinonc.2016.171>
- ⁸ H. Xiao, L. Yan, E. M. Dempsey, W. Song, R. Qi *et al.*, *Prog. Poly. Sci.*, **87**, 70 (2018), <https://doi.org/10.1016/j.progpolymsci.2018.07.004>
- ⁹ C. Eng, *Nat. Rev. Clin. Oncol.*, **6**, 207 (2009), <https://doi.org/10.1038/nrclinonc.2009.16>
- ¹⁰ P. Parashar, C. B. Tripathi, M. Arya, J. Kanoujia, M. Singh *et al.*, *Phytomedicine*, **53**, 107 (2019), <https://doi.org/10.1016/j.phymed.2018.09.013>
- ¹¹ C. C. Earle, L. N. Venditti, P. J. Neumann, R. D. Gelber, M. C. Weinstein *et al.*, *Chest*, **117**, 1239 (2000), <https://doi.org/10.1378/chest.117.5.1239>
- ¹² C. Alibert, B. Goud and J. B. Manneville, *Biol. Cell.*, **109**, 167 (2017), <https://doi.org/10.1111/boc.201600078>
- ¹³ H. B. Nair, B. Sung, V. R. Yadav, R. Kannappan, M. M. Chaturvedi *et al.*, *Biochem. Pharmacol.*, **80**, 1833 (2010), <https://doi.org/10.1016/j.bcp.2010.07.021>
- ¹⁴ U. Patil, S. Rawal, J. Pantwalawalkar, S. Nangare, D. Dagade *et al.*, *Thai J. Pharm. Sci.*, **46**, 711 (2023), <https://digital.car.chula.ac.th/tjps/vol46/iss6/11>
- ¹⁵ K. E. Wong, S. C. Ngai, K.-G. Chan, L.-H. Lee, B.-H. Goh *et al.*, *Front. Pharmacol.*, **10**, 152 (2019), <https://doi.org/10.3389/fphar.2019.00152>
- ¹⁶ F.-L. Yen, T.-H. Wu, C.-W. Tzeng, L.-T. Lin and C.-C. Lin, *J. Agric. Food Chem.*, **58**, 7376 (2010), <https://doi.org/10.1021/jf100135h>
- ¹⁷ J. Pantwalawalkar, H. More, D. Bhange, U. Patil and N. Jadhav, *J. Drug Deliv. Sci. Technol.*, **61**, 102233 (2021), <https://doi.org/10.1016/j.jddst.2020.102233>
- ¹⁸ A. A. Yetisgin, S. Cetinel, M. Zuvin, A. Kosar and O. Kutlu, *Molecules*, **25**, 2193 (2020), <https://doi.org/10.3390/molecules25092193>
- ¹⁹ S. A. Agnihotri, N. N. Mallikarjuna and T. M. Aminabhavi, *J. Control. Release*, **100**, 5 (2004), <https://doi.org/10.1016/j.jconrel.2004.08.010>
- ²⁰ V. Sabale, A. Paranjape, V. Patel and P. Sabale, *Int. J. Biol. Macromol.*, **95**, 321 (2017), <https://doi.org/10.1016/j.ijbiomac.2016.11.078>
- ²¹ P. Devkar, S. Nangare, L. Zawar, N. Shirsath, P. Bafna *et al.*, *Int. J. Biol. Macromol.*, **230**, 123360 (2023), <https://doi.org/10.1016/j.ijbiomac.2023.123360>
- ²² V. Sabale, V. Patel and A. Paranjape, *Int. J. Pharm. Investig.*, **2**, 61 (2012), <https://doi.org/10.4103/2230-973X.100039>
- ²³ N. R. Shirsath and A. K. Goswami, *Mater. Technol.*, **36**, 647 (2021), <https://doi.org/10.1080/10667857.2020.1786783>
- ²⁴ M. Biswas and S. S. Ray, in “New Polymerization Techniques and Synthetic Methodologies”, edited by M. Biswas, I. Capek, C. S. Chen, D. Mathew, C. P. Reghunadhan *et al.*, Springer-Verlag Berlin, Heidelberg, New York, 2001, pp. 167-222, https://doi.org/10.1007/3-540-44473-4_3
- ²⁵ Y. Liu and H.-I. Kim, *Carbohydr. Polym.*, **89**, 111 (2012), <https://doi.org/10.1016/j.carbpol.2012.02.058>
- ²⁶ B. Khatun, N. Banik, A. Hussain, A. Ramteke and T. Maji, *J. Microencapsul.*, **35**, 439 (2018)
- ²⁷ A. Maghsoudi, F. Yazdian, S. Shahmoradi, L. Ghaderi, M. Hemati *et al.*, *Mater. Sci. Eng. C.*, **75**, 1259 (2023), <https://doi.org/10.1016/j.msec.2017.03.032>
- ²⁸ A. K. Nayak, D. Pal and K. Santra, *Int. J. Biol. Macromol.*, **82**, 1023 (2016), <https://doi.org/10.1016/j.ijbiomac.2015.10.027>
- ²⁹ K. Dua, K. Pabreja, M. Ramana and V. Lather, *J. Pharm. Bioallied Sci.*, **3**, 417 (2011), <https://doi.org/10.4103/0975-7406.84457>